Differences in the IR Methylene Rocking Bands between the Crystalline Fatty Acids and *n*-Alkanes: Frequencies, Intensities, and Correlation Splitting

Hung-Wen Li,[†] Herbert L. Strauss,* and Robert G. Snyder*

Department of Chemistry, University of California, Berkeley, California 94720-1460

Detailed low-temperature infrared spectra in the methylene rocking−twisting progression band region from 700 to 1000 cm^{-1} are presented for the C-phase crystalline fatty acids with even numbers of carbons from 16 through 22. There are significant differences between these spectra and those of the corresponding crystalline *n*-alkanes. The differences in band frequencies, intensities, and splitting are relevant to the interpretation of infrared spectra of complex assemblies of chain molecules such as biomembranes. They are due to chain end and chain-packing differences and can be accounted for using simple models developed in earlier studies, particularly those on the *n*-alkanes. Band frequency differences result from shifts imposed on the unperturbed frequency by the end groups. Shifts associated specifically with the methyl and acid end groups were estimated from the observed frequencies of the fatty acids, fatty diacids, and *n*-alkanes and unperturbed frequencies obtained from the dispersion curve for the infinite polymethylene chain. The shifts observed for rocking band frequencies are found to be the sums of the shifts assigned to the end groups. The differences in intensity and intensity distribution can be explained using a model in which the contribution of the individual methylenes to the dipole moment derivative associated with a given band is assumed to be the same except for the terminal methylenes. These methylenes are distinguished by the adjoining chain end group. The intensity differences between a fatty acid and an *n*-alkane occur because the contribution from the acid-end methylene is much greater than that from the other methylenes. The methylene bands in the spectra of the orthorhombic and monoclinic *n*-alkanes and C-form fatty acids are split because of interchain vibrational coupling. Their splitting patterns depend on the chain tilt angle. The three different patterns can be accurately reproduced using a simple coupled oscillator model, the different tilts, and three methylene−methylene interchain interaction constants.

I. Introduction

The fatty acids are among the simplest of the lipids. Their infrared (IR) spectra, along with those of the *n*-alkanes, have features in common with the spectra of biomembranes. The spectra of both systems have been analyzed in detail, the *n*-alkanes the more so because their spectra consist mainly of bands involving the polymethylene (PM) chain, free from overlap by the characteristically intense bands associated with polar groups. Thus, the *n*-alkanes seem optimally suited for ferreting out useful relations between spectra and chain conformation. There are, however, significant differences between the spectra of the fatty acids and the *n*-alkanes spectra in the frequencies and intensities of bands associated with the methylene groups. Understanding these differences has obvious relevance to the use of vibrational spectroscopy to determine biomembrane structure and dynamics. The methylene vibrations are depicted in Figure 1.

We report here on the spectral differences associated with chain ends and chain-packing differences for the methylene rocking bands in the 700 and 1000 cm^{-1} region of the spectra of the C-phase fatty acids and the orthorhombic and monoclinic
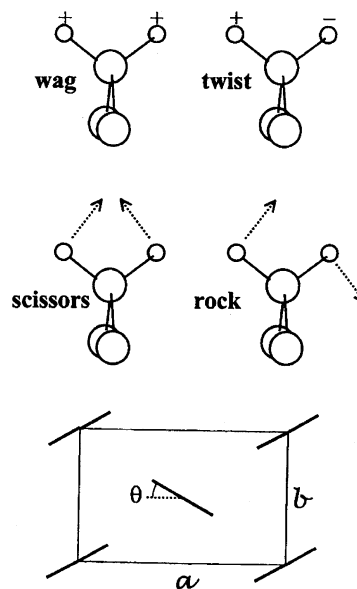

Figure 1. Methylene group vibrations, the orthorhombic perpendicular (O$_\perp$) subcell, and the setting angle θ are depicted.

n-alkanes. We consider first the effect of chain end groups and then an unexpected effect associated with chain packing. It was in fact the latter observation that initially prompted this project.

---

* Corresponding authors. E-mail: hls@cchem.berkeley.edu; r.snyder@comcast.net.
[†] Present address: Department of Biochemistry, Brandeis University, MS009, Waltham, MA 02454.
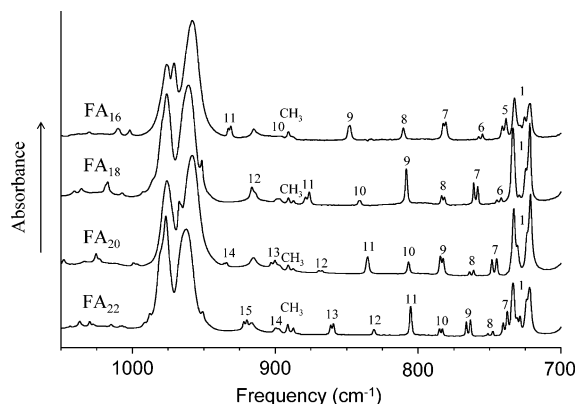
Figure 2. Methylene rocking spectra of the C-form fatty acids (FA_n, $n_{even} = 16\text{-}22$) at 10 K. The rocking band assignments (*k* numbers) and the methyl out-of-plane rocking band near 890 cm^{-1} are indicated.

It was found that the interchain band-splitting pattern displayed by the rocking bands in the IR spectrum of the C-form fatty acids was distinctly different from the patterns we had previously reported for the crystalline orthorhombic[1,2] and monoclinic *n*-alkanes[3]. Thus, initially our aim was to determine if the splitting pattern for the C-form fatty acids could be quantitatively accounted for in terms of chain tilt, which we had previously invoked to explain the patterns for the *n*-alkanes.[1-3] The principal question was whether the polar headgroup of the fatty acids would perturb the chain vibrations so as to make the simple model we had previously used inadequate. To anticipate, the fatty acid splitting can indeed be accounted by chain tilt, suggesting that the rocking band splitting pattern can be used in favorable cases to determine chain tilt in systems other than the *n*-alkanes.

In the course of analyzing the splitting pattern, other significant differences between the methylene rocking bands of the crystalline fatty acids and *n*-alkanes became evident. These include band frequency shifts, relative intensities, and intensity patterns. Accurate low-temperature spectra and previously established relations between the structural properties and vibrational spectra of the *n*-alkanes enable us to model the intrachain and interchain differences between the *n*-alkanes and fatty acids.

II. Background

A. Measurement of IR Spectra. The fatty acids (FA_n)—palmitic ($C_{16}H_{32}O_2$), stearic ($C_{18}H_{36}O_2$), arachidic ($C_{20}H_{40}O_2$), and behenic ($C_{22}H_{44}O_2$) acids—along with the corresponding alkyl methyl esters (ME_n) and the fatty diacids (di-FA_n)—hexadecanedioic ($C_{16}H_{30}O_4$) and tetratricontanedioic acids ($C_{34}H_{66}O_4$)—were purchased from Aldrich Chemical. Their purity was stated as 99%.

Thin films suitable for infrared measurements were prepared by melting a small amount of the sample onto a KBr window. After slow cooling to room temperature, the window was mounted in a closed-cycle helium refrigerator and cooled to 10 K. Infrared spectra were measured with a Nicolet 850 FTIR spectrometer at 1.0 cm^{-1} resolution and 1024 scans per spectrum. An MCT/B detector was used to cover the 450–4000 cm^{-1} range.

B. Band Progressions and Model. The IR spectra in the methylene rocking band region are shown in Figure 2 for FA16, FA18, FA20, and FA22 at 10 K. The rocking bands, whose frequencies are listed in Table 1, form the methylene rocking–twisting band progression that extends from about 720 to 1065

TABLE 1: Observed IR Frequencies of the Methylene Rocking Bands of Fatty Acids, Fatty Diacids, Alkyl Methyl Esters, and *n*-Alkanes

Frequency in cm^{-1}

	n = 16					n = 18				n = 20				n = 21		n = 22				n = 34
	FA16[a,b]		di-FA16[c]	ME16[d]	C16[e]	FA18		Me18	C18	FA20		Me26	C26	C21[f]		FA22		ME22	C22	di-FA34[c]
k	a	b				a	b			a	b			a	b	a	b			
1	732.5	721.7	722.1 / 732.8	720	721	733.6	721.7	720	722	733.1	721.2	720	720	734.2	721.5	733.5	722.1	720	721	733.3 / 721.3
5	738.4	741.0	744.5 / 747.9	757		741.9	744.8	745	740	744.9	748.3	748	737	742.8		737.5	740.3	741	731	738.9 / 742.6
6	754.9	757.6		780	767	758.2	761.1	760		761.1	763.9	763	766	765.8	760.9	747.6	751.2	751	752	754.8 / 758.5
7	780.5	782.3	(795.6)[g]	812		781.6	783.5	781	790	782.4	784.4	782				763.3	766.2	764		779.0 / 782.2
8	(810.4)[g]			849	828	(808.2)[g]		809		(806.7)[g]		808	817	807.2	806.2	782.9	784.9	783	788	(807.6)[g]
9	848.4	847.6	(870.5)[g]			841.5	840.5	842	856	(835.3)[g]		836				(805.2)[g]		806		(842.8)[g]
10	905.9	904.0										868				(831.0)[g]		832		
11	932.9	931.2	(920)[g]	933	906	878.8	876.2	878		869.4	897.2	901	880	861.9	864.4	861.1	859.1	860	842	883.2 / 881.6
12										902.7	900.3					899.7	897.5			
13				988		916.4	913.9		927	935.7	934.0	936		921.8	927.1	922.0	919.8		900	
14																				
15				1014	985							969	945							
17																				
19																				
21																				

a Fatty acids and diacids at 10 K. *b* Fatty acid components assigned from our calculations. *c* Component assignments unknown. *d* Alkyl methyl esters at 210 K. *e* *n*-Alkanes at 80 K. See also ref 10. *f* Polarization from ref 4. *g* Average frequency, splitting not resolved. Frequencies from ref 2.

Differences in IR Methylene Rocking Bands

J. Phys. Chem. A, Vol. 108, No. 32, 2004 **6631**

ORTHO n-C_n
$\Delta n = 0$

MONO n-C_n
$\Delta n = 1$
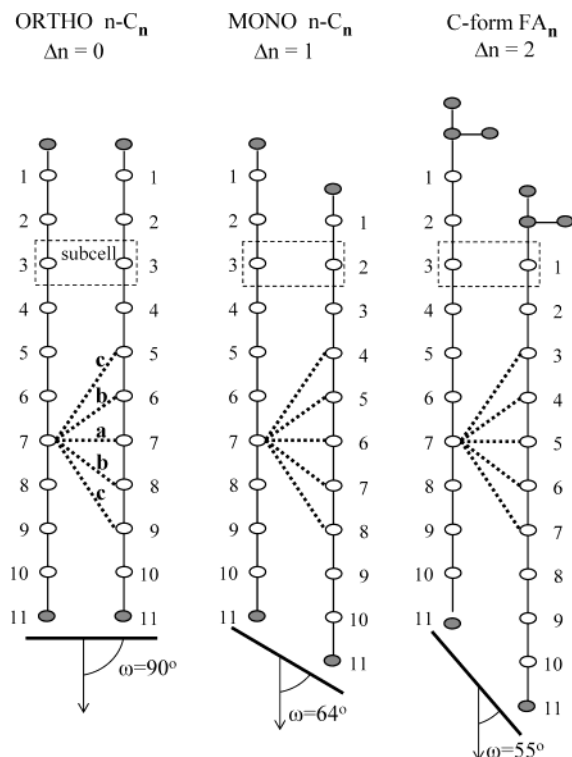
C-form FA_n
$\Delta n = 2$

Figure 3. Models of the hydrocarbon chain and chain packing for the orthorhombic and monoclinic *n*-alkanes and the C-form fatty acids. The $O_\perp$ subcell, methylene off-set number Δn, chain tilt ω, and interchain methylene–methylene interaction constants *a*, *b*, and *c* are indicated.

cm^{-1}. These bands involve both methylene rocking and twisting motions, with the ratio of rocking to twisting motion changing monotonically with frequency.[4,5] The lowest frequency band near 720 cm^{-1}, which is by far the most intense band in the progression, represents nearly pure rocking. In going to higher frequencies, the twisting contribution increases. The highest frequency band near 1065 cm^{-1} is nearly pure twisting. Because the rocking contribution to the potential energy of the vibration is, on the average, significantly greater than that for twisting, this progression is referred to as the "rocking" progression.

There is a second progression extending from 1174 to 1300 cm^{-1}, also involving methylene rocking and twisting that much resembles the rocking progression. This "twisting–rocking" progression is referred to as the "twisting" progression, because twisting rather than rocking dominates the potential energy. Its lowest frequency mode near 1174 cm^{-1} is nearly pure rocking, and its highest frequency mode near 1300 cm^{-1} is nearly pure twisting.

There are also a few bands in the spectrum of the fatty acids, some prominent, that are associated with the methyl or the acid group at the ends of the chain. Notable among them is a complex of intense bands near 970 cm^{-1}, which represents the out-of-plane deformation mode of the hydrogen in the acid group[6] and unfortunately obscures the methylene rocking bands in the 940–1000 cm^{-1} region of the fatty acid spectrum.

We have used simple models to represent both the *n*-alkane chains and their interactions with neighboring chains. As shown in Figure 3, the model chain consists of *m* identical one-dimensional harmonic oscillators that represent methylene. The oscillators are linked though nearest-neighbor coupling.[4] The vibrational frequencies ν_k and normal coordinates L_k of the vibrational modes ($k = 1, 2, 3, ..., m$) are obtained from the equations of the form

$$L^{-1} H L = \Lambda \tag{1}$$

in which *H* is defined

$$H = \begin{bmatrix} A & B & 0 & 0 & ... \\ B & A & B & 0 & ... \\ 0 & B & A & B & ... \\ 0 & 0 & B & A & ... \\ ... & ... & ... & ... & ... \end{bmatrix} \tag{2}$$

where *A* and *B* represent energies associated, respectively, with an uncoupled oscillator and nearest-neighbor coupling, Λ is a diagonal matrix whose elements are the frequency parameters λ_k, which we have defined as equal to ν_k^2, so that the λ_k have units of cm^{-2}; *L* is a symmetric orthonormal matrix whose columns are the eigenvectors L_k.

The frequency parameters of this chain are given by the equation

$$\lambda_k = A + 2B \cos \varphi_k \tag{3}$$

where φ_k, the phase difference between adjacent oscillators, is given by

$$\varphi_k = k\pi/(m + 1) \tag{4}$$

The eigenvector of mode *k*

$$L_k' = [2/(m + 1)]^{1/2} \times$$
$$[\sin \varphi_k \ \sin 2\varphi_k \ \sin 3\varphi_k \ \sin 4\varphi_k \ ... \ \sin m\varphi_k] \tag{5}$$

represents a standing wave with *k* antinodes that closely resembles the form of the normal coordinates determined from a complete vibrational analysis of all-trans *n*-alkanes.[4,5]

In our analysis, we use for eigenvectors the standing-wave forms defined by eq 5. However, for frequencies we use the observed values because those given by eq 3, which is based on our model, are not very accurate. This is evident when the two dispersion curves (ν vs φ) for the infinite PM chain shown in Figure 4 are compared. The one labeled "actual" is based on frequencies calculated using an intramolecular valence force field derived from the observed vibrational frequencies of the crystalline *n*-alkanes.[5,6] The error in these frequencies is estimated to be less than ±2 cm^{-1}. The dispersion curve labeled "model" represents eq 3 in which *A* and *B* are set to values so that the frequencies at $\varphi = 0$ and π are the same as those in the "actual" curve. Comparison with the "actual" curve shows the model-based curve to be inaccurate. Because the repeat unit for our model chain consists of a single one-dimensional oscillator, the dispersion curve based on it represents only one kind of motion, in our case, methylene rocking. In reality, there are two dispersion curves, both representing modes involving mixtures of methylene rocking and twisting. The neglect of methylene twisting is justified in part because the frequencies of the bands of interest are below 950 cm^{-1} and consequently represent modes that consist primarily of methylene rocking.[5,6]

C. Band Assignments. The systematic spacing of the progression bands found in the spectra of ordered chain molecules reflects their structural periodicity and has a practical consequence: it greatly facilitates the assignment of methylene bands. Thus, assigning the rocking bands in the spectra of the fatty acids is equivalent to numbering the bands sequentially using only odd integers. The 720 cm^{-1} band is $k = 1$, the next (higher frequency) band is $k = 3$, and so forth.
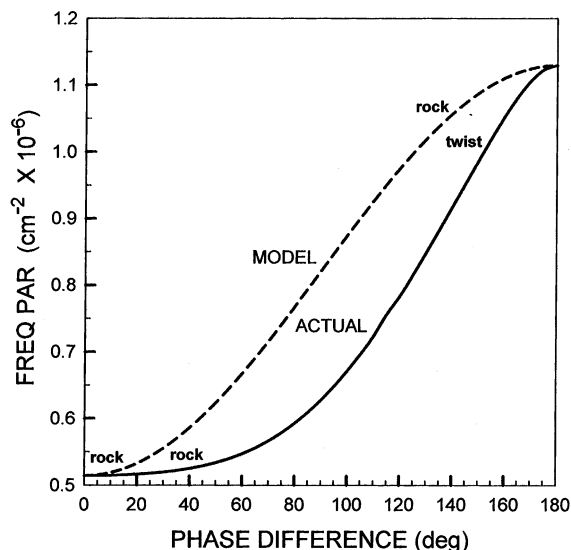
Figure 4. Dispersion curves consisting of plots of the frequency parameter λ against the phase difference φ for the infinitely long PM chain. The dispersion curve labeled "MODEL" is based on the coupled oscillator model, and the one labeled "ACTUAL" was calculated using *n*-alkane force constants derived normal coordinate calculations. The labels "rock" or "twist" indicate the type of methylene motion at the zone centers $\varphi = 0$ and 180°.

There is one complication, however. An unknown number of bands, starting with the $k = 3$ band, are hidden under the intense 720 cm^{-1} band. Nevertheless, correct numbering can be established by capitalizing on the fact that, for long chains, the frequency of a progression band is to a good approximation determined only by the phase difference of the mode. To establish the k numbering, two bands (k and k') from chains of different lengths (m and m') with (nearly) the same frequency are selected. If their frequencies are equal, it follows that their phase differences must also be equal, that is, $\varphi_{k,m} = \varphi_{k',m'}$. This equality in combination with eq 4 gives

$$k = (k' - k)(m + 1)/(m' - m) \qquad (6)$$

The value of k can be determined, since m and m' are known, and $k' - k$ can be established from the spectra of the homologous series.[4]

To determine the k values for the rocking bands of the fatty acids, we selected two bands with nearly the same frequency, but from different spectra: one is at 904 cm^{-1} in the spectrum

of FA$_{16}$, and the other is at 898 cm^{-1} in the spectrum of FA$_{22}$. Since $m = 14$, $m' = 20$, and $\Delta k = 4$, eq 6 yields $k = 10.0$. The assignments of all other rocking bands follow from this. They are listed in Table 1.

The rocking bands of the diacid, di-FA$_{34}$, were assigned in basically the same manner. The assignments for the fatty acid FA$_{18}$ were used as a reference. Because this molecule has half as many methylenes as FA$_{34}$, the spacing of the rocking modes in its spectrum is very nearly twice the spacing in the spectrum of di-FA$_{34}$. Furthermore, because all the modes for FA$_{18}$ are IR active, whereas only the k-odd modes for diFA$_{34}$ are active, the bands in the two spectra appear at nearly the same frequencies (Figure 5). If k represents a FA$_{18}$ band and k' a di-FA$_{34}$ band at the same frequency, k and k' are related as $k' = 2k - 1$. The band selected for FA$_{18}$ was the $k = 10$ band observed near 841 cm^{-1} and for di-FA$_{34}$ a band (k') observed near 843 cm^{-1}. The value of k' is therefore 19. The di-FA$_{34}$ assignments were then used as a reference in assigning the rocking bands in the spectrum of the shorter diacid, di-FA$_{18}$.

III. Chain End Group Effects: Fatty Acids versus *n*-Alkanes

A. Frequency Shifts. Marked differences are observed between the frequencies of the rocking bands of a C-form fatty acid and the corresponding (same k) bands of an *n*-alkane of the same length (see Table 1). The differences exist because the frequencies of the progression bands are affected by the chain end groups.

End group effects have previously been noted and analyzed for a number of PM chain molecules in crystals, and equations relating chain length and other factors to the end group induced frequency shifts have been reported.[7,8] We check some of these theoretical predictions using accurately measured band shifts of the rocking band frequencies for the *n*-alkanes, fatty acids, and diacids at low temperature. These molecules provide a complete set of chain end group combinations: (COOH/COOH, COOH/CH$_3$, and CH$_3$/CH$_3$) for molecules of comparable lengths.

To help in determining band shifts, we have plotted in Figure 6 the rocking band frequencies for the fatty diacids ($n = 18$, 34), fatty acids ($n = 16$, 18, 20, 22), and *n*-alkanes ($n = 16$, 18, 20, 22) against phase differences calculated from eq 4. For split bands, the average frequency is used. Figure 6 also includes the dispersion curve for the rocking−twisting vibrations for the infinitely long, all-trans PM chain. This curve is used as a
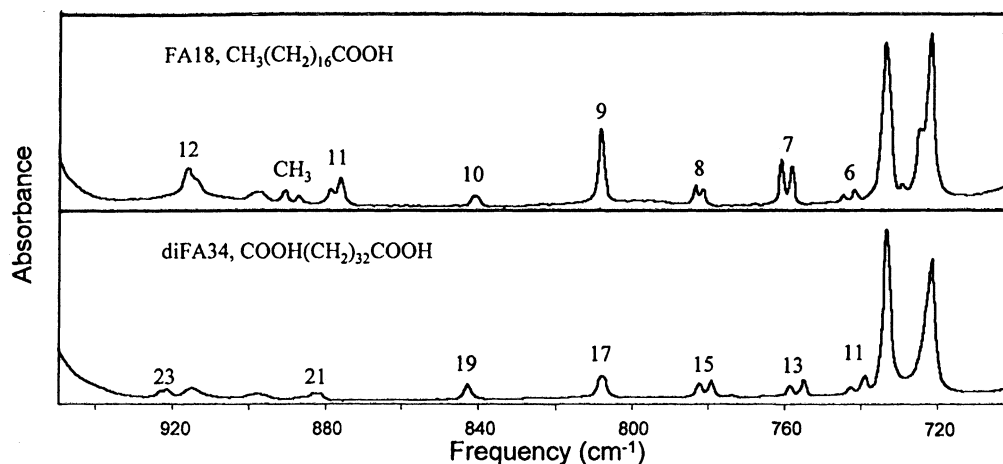

Figure 5. Methylene rocking spectra of the C-form fatty acid FA$_{18}$ and diacid di-FA$_{34}$ at 10 K. Assignments (k numbers) of the rocking bands are indicted.

Differences in IR Methylene Rocking Bands

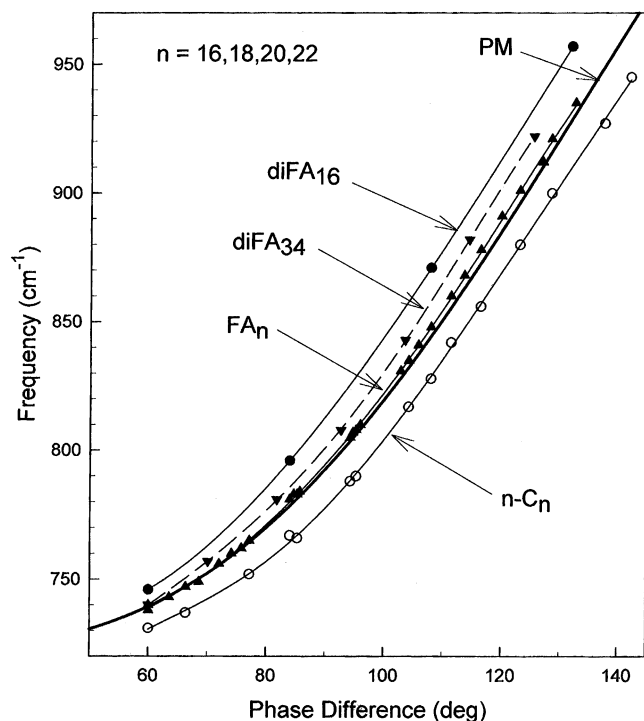*J. Phys. Chem. A, Vol. 108, No. 32, 2004* **6633**

Figure 6. Observed rocking band frequencies at 10 K for the orthorhombic and monoclinic *n*-alkanes and the C-form fatty acids with chain lengths $n_{even} = 16-22$, along with the fatty diacids di-FA$_{16}$ and di-FA$_{34}$, plotted against the phase difference calculated from eq 4. The experimentally based dispersion curve for the infinite PM chain is included as a reference.

reference since end effects are absent. Thus, we have defined a band shift $\Delta\nu_\varphi$ as $\Delta\nu_\varphi = \nu_\varphi^{obsd} - \nu_\varphi^{PM}$, where φ is the phase difference given by eq 4, ν_φ^{obsd} is the observed frequency, and ν_φ^{PM} is the unshifted frequency at φ given by the PM dispersion curve.

Frequency shifts due to chain end group interactions are predicted to be proportional to $1/(m + 1)$, where *m* is the number of methylene groups.[7] This relation accounts for the relative frequency shifts of the rocking bands measured for the diacid di-FA$_{34}$ and di-FA$_{16}$. The end group shift for di-FA$_{34}$ is found to be about half that for di-FA$_{16}$ (Figure 6). The shift ratios (di-FA$_{34}$ to di-FA$_{16}$) at phase differences of 80, 100, and 120° (corresponding to frequencies of roughly 800, 850, and 900 cm^{-1}) are 0.44, 0.44, and 0.63, the average being 0.50. The calculated value of this ratio, assuming the shifts are proportional to $1/(m + 1)$, is 0.52, very near the experimentally derived value.

In our frequency-phase plots for the fatty acids and *n*-alkanes shown in Figure 6, we find little evidence of a systematic "drift" with chain length in going from 14 to 20 methylenes. In going from 14 to 20 methylenes, the shift variation, according to the $1/(m + 1)$ relation, is between 1 and 2 cm^{-1} for the *n*-alkanes, which is too small to observe. For the fatty acids, the calculated variation is smaller, less than 1 cm^{-1}, since the shift (4 cm^{-1}) is much smaller than the 12 cm^{-1} shift for the *n*-alkanes.

Theory also indicates that the chain end groups contribute independently to the shift.[7] Our measurements support this. We have observed that the end group shifts for the fatty acids are small relative to shifts for diacids and *n*-alkanes. The shifts for the diacids and *n*-alkanes are comparable in magnitude and opposite in sign. Therefore, when combined, they largely cancel. In quantitative terms, the average shift for the *n*-alkanes is -16 ± 3 cm^{-1}, and for the diacids it is 22 ± 6 cm^{-1}. The predicted value for the fatty acids is the average of these, that is, about 3 ± 3 cm^{-1}. The observed shift is less than 4 cm^{-1}.

It is known from earlier normal coordinate calculations that the end group shifts for the *n*-alkanes result from coupling between methylene rocking and methyl out-of-plane rocking.[5] The coupling between the adjacent methyl and methylene groups is similar to that between adjacent methylenes. Therefore, the presence of methyl groups has an effect similar to increasing the number of methylenes, that is, a reduction in the frequencies of the rocking bands for a given value of *k*.

We suggest that the acid group reduces vibrational coupling between the two neighboring methylenes nearest the acid group, relative to the coupling between two interior methylenes, and therefore causes some degree of vibrational isolation of the methylene adjoining the acid group. This will reduce the effective length of the chain and produce an increase in the rocking band frequencies. Decreased coupling between the two methylenes would occur if the acid group induced a change in the rocking force constant of the end methylene group.

It is noteworthy that the frequencies and, consequently, the frequency shifts of the rocking bands in the spectra of the alkyl methyl esters (ME$_n$, $n = 16$, 18, 20, 22) are essentially the same as those for the fatty acids (Table 1). Figure 7 shows that the bands in the spectra of the $n = 20$ ester and fatty acid have nearly the same frequencies. The similarity indicates that the C(O)O group alone is responsible for the frequency shifts. The hydrogen of the acid group and the methyl of the ester group are apparently too remote to have an appreciable effect.

B. IR Intensities. *1. Observations and Measurements.* There are similarities and differences between the fatty acids and *n*-alkanes in the intensities and intensity patterns of their methylene rocking bands. These are in evidence in the intensity-normalized IR spectra of FA$_{20}$ and *n*-C$_{21}$ shown in Figure 8. The spectra are alike in that the $k = 1$ band near 720 cm^{-1} is by far the most intense band. Moreover, the intensity of this band is nearly the same in both spectra. Another similarity is that, in going to higher frequencies, the intensities of the *k*-odd bands die out around 1000 cm^{-1}.

A major difference is that, except for the $k = 1$ band at 720 cm^{-1}, the rocking bands of the fatty acids are much more intense. The distribution of intensity is also quite different. In going to higher frequencies, the intensities of the *k*-odd bands of the fatty-acid first increase, whereas those for the *n*-alkanes decrease. The fatty acid intensities reach a maximum value around 800 cm^{-1} and thereafter decrease monotonically. As to the *k*-even bands, they are totally absent in the *n*-alkane spectra, but are present for the fatty acids due to lower molecular symmetry. In going to higher frequencies, the *k*-even band intensities change in the same manner as those for the *k*-odd bands; that is, they increase with frequency until a maximum is reached near 800 cm^{-1} and then decrease to near zero near 1000 cm^{-1}. The intensities of the *k*-even bands for the fatty acids are, however, significantly lower than those of the *k*-odd bands.

These intensity differences are nearly all accountable for the differences in the chain end groups. We note, however, that the influence of the end groups on the intensities is indirect. Because it participates in the chain vibrations, it is the methylene group adjoining the end group, whose electronic properties are modified by the end group, that is most responsible for the differences.

The measured IR intensities, A_k, of the rocking bands, reduced to a common but not absolute scale, are listed in Table 2 for the fatty acids and the *n*-alkane *n*-C$_{21}$. The intensities for each fatty acid were scaled to each other using as an internal standard the summed intensities of the two acid-group bands at 694 and
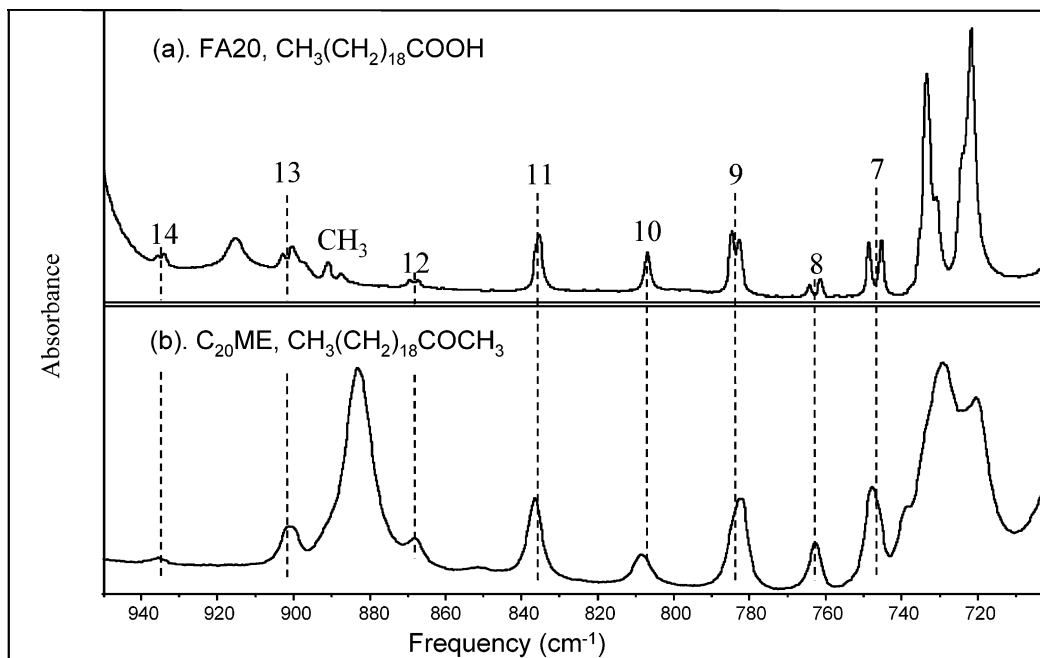
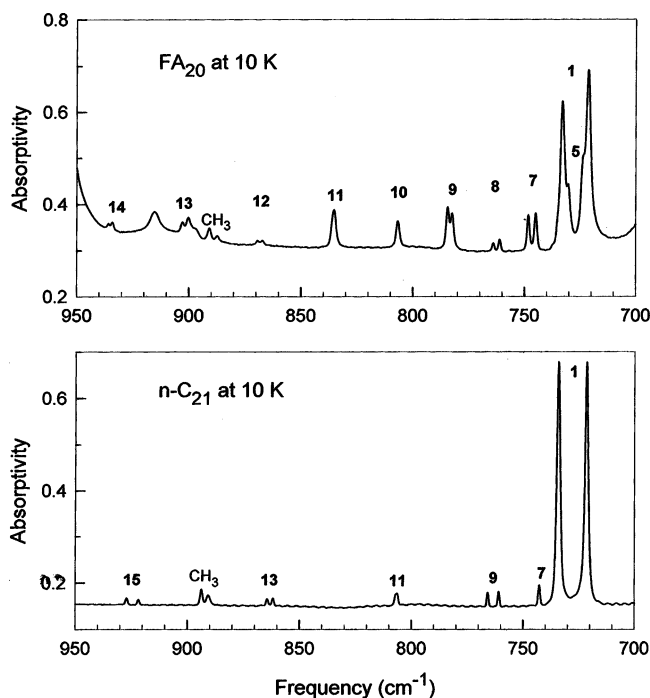**Figure 7.** Methylene rocking spectra of the C-form fatty acid FA_{20} at 10 K and the alkyl methyl ester ME_{20} at 232 K.

Figure 8. Methylene rocking spectra of the C-form fatty acid FA_{20} and the orthorhombic *n*-alkane *n*-C_{21} at 10 K shown on a common intensity scale.

672 cm^{-1}. The *n*-alkane *n*-C_{21} intensities were scaled to the fatty acid intensities using as a reference the summed intensities of the pair of nominally degenerate methyl CH stretching bands at 2962 and 2952 cm^{-1}. The uncertainty in the measured intensities is estimated to be around 20%.

Our intensity analysis is based on dipole moment derivatives rather than on intensities because the equations relating dipole derivatives to parameters associated with our model are then linear. The dipole moment derivatives and intensities are related as

$$\partial\mu/\partial Q_k = \pm K A_k^{1/2} \qquad (7)$$

where Q_k is the normal coordinate for the *k*th rocking mode and *K* is a constant. The relative magnitudes of the $\partial\mu/\partial Q_k$ for the rocking bands of C-form fatty acids and the *n*-alkane, *n*-C_{21}, all measured at 10 K, are plotted in Figure 1S of the Supporting Information against the phase difference estimated using eq 4. The phase differences can be converted to frequencies though the PM dispersion curve in Figure 4. Figure 1S shows that the intensities of the fatty acids are considerably greater than those of the alkanes and vary in a nonmonotonic manner.

The dipole derivatives for the *n*-alkanes can be treated as scalar quantities, since the directions of rocking-mode dipole derivatives must be perpendicular to the symmetry plane defined by the skeletal carbons. To simplify our calculations, we have assumed this is true also for the fatty acids.

2. The Group Moment Model. Our analysis is based on the "group moment" model we previously employed to interpret the intensities of the IR bands of the all-trans *n*-alkanes, *n*-C_4H_{10} through *n*-C_8H_{18}.[11] In this model, the dipole moment derivative $\partial\mu/\partial Q_k$ is expressed as the sum of contributions from the individual methylenes that make up the chain. Such a model is well-suited to nonpolar, saturated chains with a repeat unit consisting of simple groups, preferably ones having a high degree of symmetry. The methylene group is especially well-qualified in this respect. The contribution of a given methylene group to $\partial\mu/\partial Q_k$ is given by the product of the methylene rocking group dipole-moment derivative and a factor indicating the degree to which the methylene participates in the *k*th mode. The group moment derivative is designated $\partial\mu/\partial S_i$, and the weighting factor is $\partial S_i/\partial Q_k$, where S_i is the group rocking coordinate for the *i*th methylene. The dipole moment derivatives (eq 7) expressed in terms of group coordinates S_i are

$$D_{km} = C[\sum_{i=1}^{m}\partial\mu/\partial S_i\cdot\partial S_i/\partial Q_k] \qquad (8)$$

or, more concisely,

$$D_{km} = C[\sum_{i=1}^{m}M_i L_{ik}] \qquad (9)$$

TABLE 2: Relative IR Intensities and Band Splitting of the Methylene Rocking Bands Measured for the Fatty Acids and n-C$_{21}$ at 10 K

k	FA$_{16}$			FA$_{18}$			FA$_{20}$			FA$_{22}$			n-C$_{21}$		
	$\nu_k{}^a$	$A_k{}^b$	$\Delta\nu_k{}^{a,c}$	ν_k	A_k	$\Delta\nu_k$	ν_k	A_k	$\Delta\nu_k$	ν_k	A_k	$\Delta\nu_k$	ν_k	A_k	$\Delta\nu_k$
1	727	$(2.1)^d$	10.8	728	$(2.4)^e$	11.9	727	$(2.7)^f$	11.9	728	$(1.9)^f$	11.4	727	$(2.4)^f$	12.7
5	740	0.34	−2.6												
6	756	0.09	−2.7	743	0.05	−2.9									
7	781	0.47	−1.8	760	0.28	−2.9	747	0.26	−3.4	739	0.16	−2.8	740	0.100	
8	810	0.17	$(0)^f$	783	0.13	−1.9	762	0.06	−2.8	749	0.04	−3.6			
9	848	0.30	0.8	808	0.35	(0)	783	0.31	−2.0	765	0.22	−2.9	763	0.059	4.9
10	905		1.9	841	0.06	1.0	807	0.13	(0)	784	0.10	−2.0			
11	932		1.7	878	0.08	2.6	835	0.22	(0)	805	0.28	(0)	807	0.046	1.0
12				915		2.5	868	0.04	1.1	831	0.06	(0)			
13							901	0.07	2.4	860	0.17	2.0	863	0.041	−2.6
14							935	0.04	1.7	899		2.2			
15										920	0.04	2.2	924	0.031	−5.3

^{a} Frequency in cm^{-1}. ^{b} Relative integrated IR intensities. ^{c} Splitting defined as $\nu_k{}^a - \nu_k{}^b$. Sign determined from our calculations. ^{d} Includes bands $k = 1-4$. ^{e} Includes band $k = 1-5$. ^{f} Includes bands $k = 1-6$. ^{g} Too small to measure; probably 1.0 cm^{-1}.

where D_{km} designates $\partial\mu/\partial Q_k$ for a molecule of m methylenes, and M_i is the ith group moment derivative $\partial\mu/\partial S_i$. In eq 9, the eigenvector element L_{ik} has replaced $\partial S_i/\partial Q_k$, since $S_i = \sum_{k=1}^{m} L_{ik}Q_k$. This follows from the relation $\mathbf{S} = \mathbf{LQ}$, where $\mathbf{S}$ and $\mathbf{Q}$ are column vectors that represent, respectively, the group coordinates and the normal coordinates expressed in terms of group coordinates.[12] The L_{ik} elements, which are defined in eq 5, are given by $L_{ik} = h_m \sin i\varphi_k$, where h_m is the normalization factor $[2/(m + 1)]^{1/2}$.

The group moment derivatives M_i can also treated as scalars, because the symmetry of the methylene group (point group C_{2v}) is congruent with the local symmetry of the carbon skeleton. As a result, the group moment derivative vectors are also perpendicular to the skeletal plane.

Upon incorporating the above-defined quantities, eq 9 can be rewritten

$$D_{km} = Ch_m X_k \left[\left\{\left(\sum_{i=1}^{m} \sin i\varphi_k\right) - \sin\varphi_k - \sin m\varphi_k\right\}M_0 + \sin\varphi_k M_1 + \sin m\varphi_k M_m\right] \quad (10)$$

where M_0 is the group moment derivative associated with the interior methylenes, and M_1 and M_m represent the chain end methylenes. The quantity X_k in eq 10 represents the fraction of the normal coordinate k associated with methylene rocking. This factor is necessary because the normal coordinates involve both rocking and twisting. (By virtue of the symmetry of the methylene group, twisting does not contribute any significant intensity.) Lacking normal coordinates, we have used for X_k the fraction of the potential energy associated with methylene rocking. This quantity equals $L_{ik}^2 F_{ii}/\lambda_k$, where F_{ii} is the methylene rocking force constant.[5] In Figure 2S, the fraction X_k is plotted as a function of the phase difference. The figure shows a smooth variation of X_k from 1 at 0° difference to near zero at 180°.

Equation 10, rewritten to apply specifically to the k-odd modes, is

$$D_{km} = C_{km}[(\cot\varphi_k/2)M_0 + \sin\varphi_k(M_1 + M_m - 2M_0)] \quad (11a)$$

For the k-even modes we have

$$D_{km} = C_{km}[\sin\varphi_k(M_1 - M_m)] \quad (11b)$$

In these equations, C_{km} replaces $Ch_m X_k$ in eq 10, and $\cot\varphi_k/2$ replaces $\sum_{i=1}^{m} \sin i\varphi_k$.

3. Origin of the Intensity Patterns. The main features of the observed methylene rocking band intensity (or, more correctly, the dipole moment derivative) patterns observed in the IR spectra of the n-alkanes and fatty acids are accounted for by eqs 11a and 11b. The trigonometric functions, $\cot\varphi_k/2$ and $\sin\varphi_k$, which originate from the standing-wave representations of the normal coordinates, determine the overall intensity pattern. The group moment derivatives, M_1, M_m, and M_0, in various combinations serve to scale the intensities of the k-odd and the k-even bands.[2]

The value of D_{km} for k-odd bands given by eq 11a involves two terms. The first represents the contribution from the internal methylenes. This contribution is quantitatively the same for both the n-alkanes and fatty acids. Because it is proportional to $\cot\varphi_k/2$, the $k = 1$ rocking mode at 720 cm^{-1} is the most intense band in the progression by virtue of having by far the smallest phase difference φ_k and, therefore, by far the greatest value of $\cot\varphi_k/2$. With increasing frequency (and therefore increasing φ_k), the interior methylene contributions drop off rapidly. The contribution from the end methylenes, given by the second term in eq 11a, is relatively small for the n-alkane because the dipole derivatives, M_1 and M_m, which by symmetry are equal, have values not markedly different from that of interior methylene derivative, M_0. As a result, the factor, $M_1 + M_m - 2M_0$, is relatively small. Eq 11a predicts that the intensities of the rocking progression bands for the n-alkanes, starting with the intense $k = 1$ band at 720 cm^{-1}, will rapidly diminish in going to higher frequencies, which is what is observed. It is notable that the $k = 1$ band at 720 cm^{-1} is unique in that its intensity is virtually independent of the headgroup. This is because its intensity comes almost exclusively from the internal methylenes.

The intensities and intensity patterns for the k-odd bands of the fatty acids differ from those for the n-alkanes mainly because the dipole derivative M_0 associated with the end methylene next to the acid group is much larger in magnitude than M_1 or M_m. The quantity, $M_1 + M_m - 2M_0$, therefore plays a much more significant role in determining intensities than it did for the n-alkanes. The coefficient of this factor, $\sin\varphi_k$, increases with φ, until it reaches a maximum value at 90°. This phase difference corresponds to about 800 cm^{-1}. An intensity maximum is indeed observed near 800 cm^{-1}.

Equation 11b, which applies to the k-even bands, consists of a single term that involves only the chain end methylenes. Their intensity contribution is equal to the product of the difference between the two end methylene derivatives ($M_1 - M_m$) and $\sin\varphi_k$. Because $M_1 = M_m$ for the n-alkanes, $M_1 - M_m$ is zero, and hence, no k-even bands appear. In contrast, $M_1 - M_m$ for the
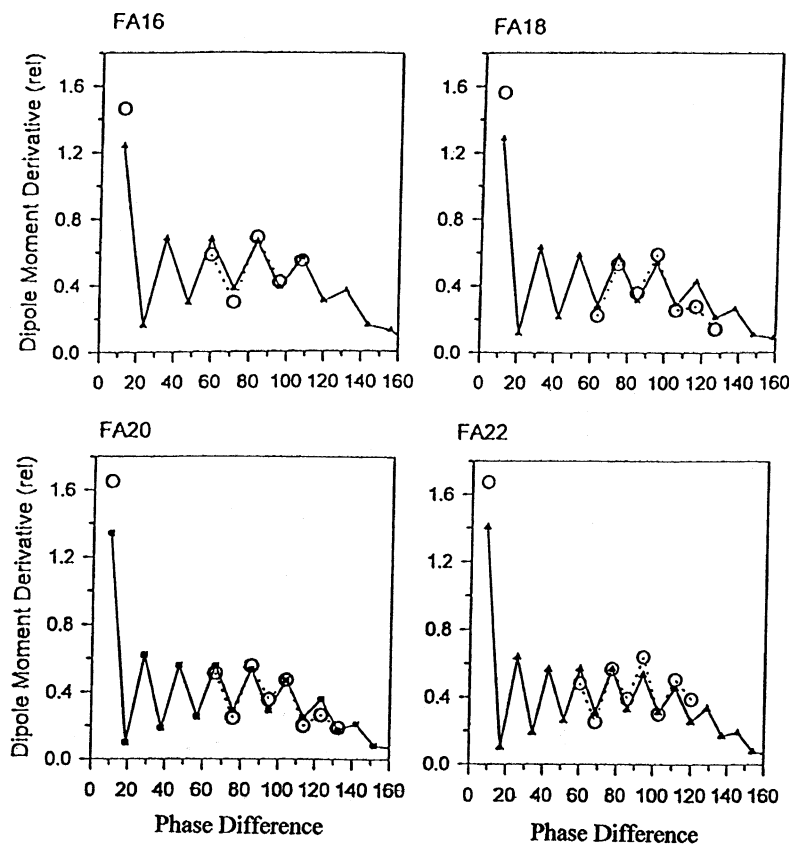
Figure 9. Observed and calculated dipole moment derivatives for the rocking bands of the fatty acids at 10 K, plotted against the phase difference. ○ indicates observed values. ▲ indicates values calculated with $M_0 = 1$, $M_m = 1.63$, and $M_1 = 5.0, 4.5, 4.5, 5.0$ for $n = 16, 18, 20, 22$, respectively.

fatty acids is large. The $\sin \varphi_k$ factor ensures an intensity maximum near 800 cm^{-1} for the k-even bands, as it did for the k-odd bands. Again, this is what is observed.

4. Evaluation of the Methylene Group Moment Derivatives. We have estimated the relative values of M_0, M_1, and M_m from the dipole moment derivatives measured for n-C$_{21}$ and the fatty acids. This was achieved by adjusting the group moment parameters to give an optimum fit between the measured D_{km} and their values calculated from eqs 11a and 11b. Since the measured values are relative, we can set $M_0 = 1$. For comparison with the observed D_{km}, the calculated D_{km} values were scaled using a factor adjusted so that the calculated intensity of the 720 cm^{-1} band in the spectrum of n-C$_{21}$ equaled the observed intensity. The 720 cm^{-1} band was used because its intensity is uniquely high and can therefore be accurately measured, and because, as previously noted, its value is nearly independent of the end groups.

Our results for the n-alkane n-C$_{21}$ are summarized in Figure 3S, where the observed values of the D_{km} are displayed along with values obtained from two different calculations. In one case we assumed the methylenes were identical; that is, $M_0 = M_1 = M_m = 1$. Under this assumption, the calculated D_{km} decreased somewhat too rapidly with increasing frequency. This was remedied in the second calculation by increasing M_1 (= M_m) to the optimal value of 1.63 ± 0.05, a value substantially larger than that for the interior methylenes ($M_0 = 1.0$). The contribution of an end methylene to the rocking band intensity was found to exceed that from an interior methylene by a factor of about 2.7, or, stated differently, the contribution from the two end methylene groups represents about 24% of the overall intensity.

In fitting the fatty acid dipole derivatives, we kept the group moment derivatives M_0 and M_m at their n-C$_{21}$ values (1.00 and

1.63) and varied the acid end methylene group moment, M_1, in steps of 0.05 for each of the four fatty acids. The values of M_1 that gave the best fit for the $n = 16, 18, 20, 20$, and 22 fatty acids are 5.0, 4.5, 4.5, and 5.0, respectively. As indicated in Figure 9, the calculated and measured D_{km} values are generally in good agreement. The contribution of acid end methylene to the intensity is large. On the basis of the average value determined for M_1 (4.8 ± 0.5), it exceeds that from an interior methylene by a factor of about 23 and accounts for about 55% of the total rocking intensity.

Figure 10 shows simulated "stick" spectra for FA$_{20}$ and n-C$_{21}$ to be compared with the corresponding measured spectra in Figure 8. Taking into account the effect of the band splitting in the observed spectrum, the intensities and intensity distribution for the rocking bands in the calculated spectra are found to correspond fairly well to the observed. We note that the calculated spectrum shows the bands on the high-frequency side of the 720 cm^{-1} band that are totally obscured in the measured spectrum.

IV. Band Splitting

A. Background. "Correlation" or "factor group" splitting of the intense methylene scissoring and rocking bands at 1465 and 720 cm^{-1} is frequently a prominent feature in the IR spectra of crystals of PM chain molecules and polymers. This splitting, which is of the order of 10 cm^{-1}, is observed if the subcell that defines the local chain-packing geometry[13] is orthorhombic-perpendicular (O$_\perp$), as is the case for the systems studied here. The O$_\perp$ subcell, shown in Figure 1 as viewed along the chain direction, contains two chains whose skeletal planes are approximately at right angles to each other. Because of interchain vibrational interaction and hence, coupling, the in-phase and
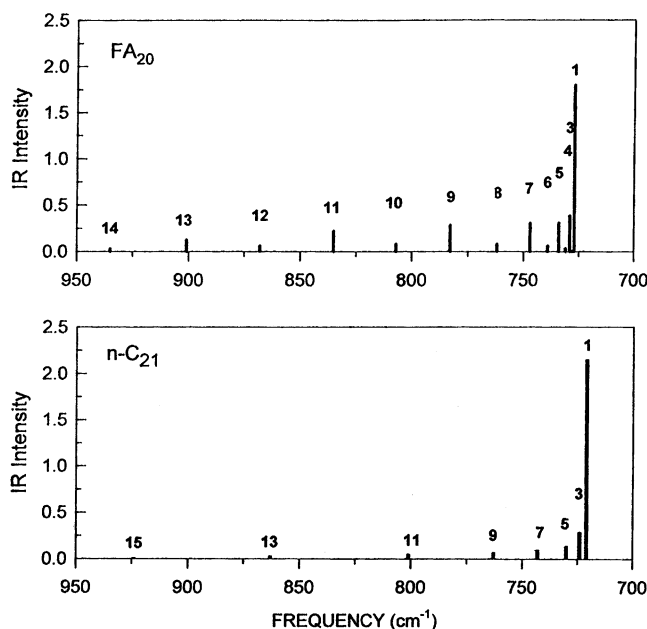
Differences in IR Methylene Rocking Bands

J. Phys. Chem. A, Vol. 108, No. 32, 2004 **6637**

Figure 10. Rocking band "stick" spectra of FA$_{20}$ and c-C$_{21}$ drawn using observed frequencies and calculated intensities. The intensities for FA$_{20}$ were obtained with M_0, M_1, and M_m equal to 1, 4.5, and 1.63, and those for *n*-C$_{21}$ with M_0, M_1, and M_m equal to 1, 1.63, and 1.63. The intensities have common scale values.

out-of-phase vibrations involving the two chains have slightly different frequencies. This gives rise to two bands and, hence, the apparent splitting.

Detailed selection rules for the vibrations associated with odd-numbered *n*-alkanes that make up the orthorhombic crystal structure reported by Smith[14] for *n*-C$_{23}$ are discussed in ref 2. The chains in this crystal are perpendicular to the lamellar plane. The crystallographic orthorhombic unit cell, not to be confused with the "orthorhombic" subcell, extends over two layers and contains four molecules, two in each layer. The selection rules based on this structure predict that each IR methylene rocking, twisting, and scissoring band will have two components. For the rocking modes, however, selection rules based on a single layer are adequate since lateral interactions between neighboring chains in the same layer are much stronger than those between chains in different layers.

The splitting observed for the PM chains, first reported in ref 15, results from short-range interchain vibrational coupling.[2,16,17] Because the coupling is short-ranged, its effects have led to a number of IR methods used to probe structure. A ready example is our utilization of its influence on band shape for mixtures of perdeuterated and perhydrogenated chains for the purpose of determining and monitoring phase separation in multicomponent PM chain systems. In application to binary mixtures, one of the two components is perdeuterated. Because significant vibrational, interchain coupling can occur only between pairs of isotopically alike chains, the shapes of the CH$_2$ and CD$_2$ scissors and rocking bands are sensitive to like-chain aggregation. We have exploited this sensitivity to measure aggregation and phase separation in crystalline *n*-alkane,[18] alkyl ester,[19] and phospholipid bilayer[20] mixtures.

In keeping with above-mentioned selection rules, not only is the 720 cm^{-1} rocking band split but all the other methylene rocking bands in the 720–1000 cm^{-1} region of the IR spectra of the orthorhombic and monoclinic *n*-alkanes as well. Splitting, like band frequency, is a function of the phase difference associated with the vibrational mode involved.[1–3,9] The numerous splitting data thus provided have enabled estimations of

the interchain force constants. The interchain constants derived from the splittings compare well with values estimated from known H···H repulsive potentials.[2] In a comprehensive calculation, Tasumi and Shimanouchi[17] used interchain force constants based on H···H repulsion potentials that were evaluated from selected splittings to calculate a complete set of dispersion curves for the orthorhombic PM crystal. The calculated splittings for internal vibrational modes and for frequencies of external modes (lattice vibrations) are generally in good agreement with measured values.

For the orthorhombic *n*-alkanes, the components of split bands can be distinguished by their polarization, determined from IR measurements on oriented single crystals. Selection rules indicate that one component will be polarized along the *a*-axis of the unit cell and the other along the *b*-axis. For the orthorhombic *n*-alkanes, the unit cell axes *a* and *b* coincide with the a_s and b_s axes of the subcell (Figure 1). This is not the case for the monoclinic *n*-alkanes and the C-form fatty acids. Since the three systems considered have a common subcell, the split band components are assigned with reference to the a_s or the b_s axis. (To assign a band component to an in-phase or out-of-phase mode requires the terms "in-phase" and "out of phase" to be explicitly defined. See ref 2.)

Chain tilt can complicate polarization measurements because, as noted, the a_s and b_s axes differ from the *a* and *b* axes. However, this is not a serious problem for the monoclinic *n*-alkanes because the tilt is relatively small. For the fatty acids, there is a more serious problem due to the low symmetry of the molecule and highly polar character of the acid headgroup. As a result, the polarization directions of a split component for the fatty acids vary depending on the normal coordinate of the mode. Consequently, polarization measurements are not very useful for establishing assignments. They can, however, be established through calculations to be described.

The chain-packing geometries for the orthorhombic and monoclinic *n*-alkanes and the C-form fatty acids are nearly identical, except for the chain tilt angle. As noted, all three systems have O$_\perp$ subcells. For the orthorhombic and monoclinic *n*-alkanes, the lateral subcell dimensions are $a_o = 7.41$ Å and $b_o = 4.96$ Å,[21] and for the fatty acids, $a_o = 7.34$ Å and $b_o = 4.96$ Å.[21] The tilt angle for the orthorhombic *n*-alkanes is 90°,[14] for the monoclinic *n*-alkanes it is 64°,[21] and for the C-form fatty acids it is 55°.[22]

B. Equations for Band Splitting. Interchain splitting is defined in terms of frequency as $\Delta\nu_k = \nu_k^a - \nu_k^b$ and in terms of frequency parameter as $\lambda_k = \lambda_k^a - \lambda_k^b$. The splitting may be plus or minus. For the *n*-alkanes, the signs follow from the band components assignments. For the fatty acids, the signs were established from calculations to be described.

In our analysis, it is convenient to express chain tilt in terms of the longitudinal displacement between the two chains in the unit cell associated with a single layer. The displacement is measured in terms of number of methylenes, Δn, referred to as the "off-set" number. Thus, $\Delta n = 1$ indicates that one of the two chains in the unit cell is displaced relative to the other by one methylene. (We note that longitudinal chain translation of an odd number of methylenes involves a concurrent chain rotation of 180°.) Figure 3, which emphasizes the translational aspect by showing the chains aligned vertically, depicts chain packing for off-set numbers of 0, 1, and 2, corresponding to orthorhombic and monoclinic *n*-alkanes, and the C-form fatty acids.

The interaction between the two chains in the repeat unit is assumed to be the sum of local interactions between methylenes

on neighboring chains. Three interchain methylene−methylene force constants, designated a, b, and c, are shown in Figure 3. They correspond to interchain interactions between nearest-neighbor methylenes in the same plane, in nearest-neighboring planes, and in next nearest-neighboring planes.

The interaction between the two chains in the unit cell is expressed

$$H = \begin{bmatrix} H^0 & 2h \\ 2h' & H^0 \end{bmatrix} \qquad (12)$$

where H°, previously defined in eq 2, represents an isolated chain. The elements of the interchain-coupling matrix h consist of linear combinations of the methylene−methylene coupling constants a, b, and c. The factor of 2 in front of the off-diagonal elements reflects the two-dimensional character of the chain−chain interactions in the layer.

Since the splitting of the rocking progression bands is normally small (<15 cm^{-1}) relative to the frequency separation between successive $(k, k + 1)$ rocking modes, H can be separated into in-phase and out-of-phase components. Using the transformation matrix

$$T = \frac{1}{\sqrt{2}} \begin{bmatrix} 1 & 1 \\ 1 & -1 \end{bmatrix} \qquad (13)$$

we obtain

$$THT = \begin{bmatrix} H^\circ + 2h^s & 2h^d \\ -2h^d & H^\circ - 2h^s \end{bmatrix} \qquad (14)$$

where $h^s = (h' + h)/2$ is symmetric, and $h^d = (h'-h)/2$ is antisymmetric. The effect of h^d is to perturb the frequencies of the in-phase and out-of-phase band components and to mix their eigenvectors. However, h^d can in general be ignored because its elements are small relative to those of H°, and its contribution is only second order. Then we have

$$H^a = H^\circ + 2h^s \qquad (15a)$$

$$H^b = H^\circ - 2h^s \qquad (15b)$$

where a and b superscripts identify the component vibrations.

The frequency parameters for the a and b components are the eigenvalues of H^a and H^b. These are

$$\lambda_k{}^a = \lambda_k{}^0 + 2\sum_{i=1}^{m-1} h_i^s \cos i\varphi_k \qquad (16a)$$

$$\lambda_k{}^b = \lambda_k{}^0 - 2\sum_{i=1}^{m-1} h_i^s \cos i\varphi_k \qquad (16b)$$

so that the splitting is

$$\Delta\lambda_k = 4\sum_{i=1}^{m-1} h_i^s \cos i\varphi_k \qquad (17)$$

Explicit equations for the splitting are obtained upon substituting into eq 17 the expression for h^s that is defined in connection with eq 14. It is convenient to represent the symmetric band matrixes h and h^s by a sequential list of the elements of an untruncated row of the matrix. The sequence begins with the first nonzero element and ends with the last such element. The diagonal element is underlined. Thus, H° in
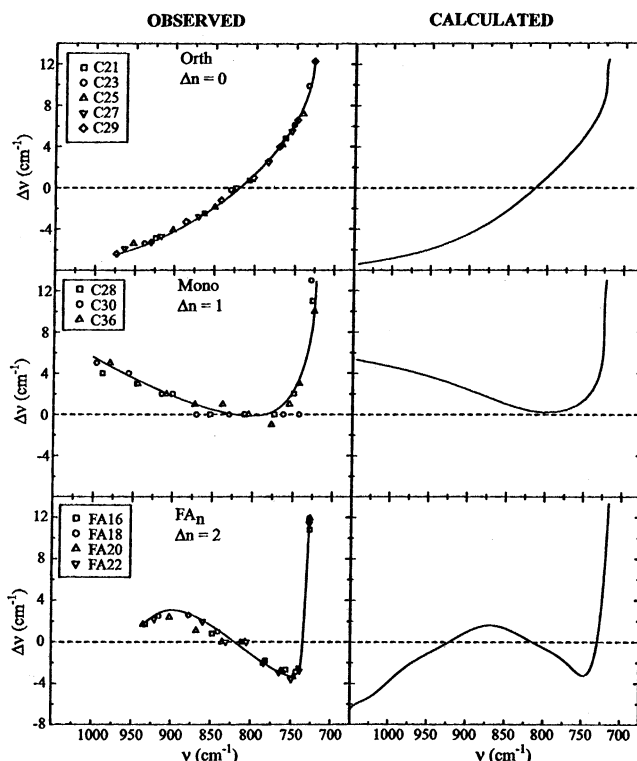

Figure 11. Observed and calculated splitting $\Delta\nu_k$ of the methylene rocking bands for the orthorhombic and monoclinic n-alkanes and the C-form fatty acids, plotted against band frequency. The data points in the observed splitting plots were "spline-fitted" to indicate the splitting patterns. The calculated curves were obtained from eqs 19a−c using values for the coupling constants a, b, and c derived from the observed splittings obtained through least-squares fitting (Table 3).

eq 2 is represented as M_B $(B,\underline{A},B\}$, where M_B stands for "band matrix". The h and h^s matrixes for each system are listed below.

Orthorhombic n-C$_n$ ($\Delta n = 0$):

$$h = M_B\{c, b, \underline{a}, b, c\} \; h^s = M_B\{c, b, \underline{a}, b, c\} \qquad (18a)$$

Monoclinic n-C$_n$ ($\Delta n = 1$):

$$h = M_B\{b, a, \underline{b}, c\} \; h^s = {}^1/{}_2 M_B\{c, b, a + c, \underline{2b}, a + c, b, c\} \qquad (18b)$$

C-form FA$_n$ ($\Delta n = 2$):

$$h = M_B\{c, b, a, b, \underline{c}\} \; h^s = {}^1/{}_2\, M_B\{c, b, a, b, \underline{2c}, b, a, b, c\} \qquad (18c)$$

The splitting equations are then

$$\Delta\lambda_k^{\Delta n=0} = 4[a + 2b \cos \varphi_k + 2c \cos 2\varphi_k] \qquad (19a)$$

$$\Delta\lambda_k^{\Delta n=1} = 4[a \cos \varphi_k + b(1 + \cos 2\varphi_k) + c(\cos \varphi_k + \cos 3\varphi_k)] \qquad (19b)$$

$$\Delta\lambda_k^{\Delta n=2} = 4[a \cos 2\varphi_k + b(\cos \varphi_k + \cos 3\varphi_k) + c(1 + \cos 4\varphi_k)] \qquad (19c)$$

C. Results. *1. Observed Splitting and Splitting Patterns.* In Figure 11 to the left, the measured band splittings for the n-alkanes and fatty acids are plotted against band frequency. Spline-fitted curves are included to suggest the shapes of the plots. The values of the splittings used for the orthorhombic n-alkanes $n_{odd} = 21-29$ at 77 K are from ref 2. Those for the

Differences in IR Methylene Rocking Bands

J. Phys. Chem. A, Vol. 108, No. 32, 2004 **6639**

TABLE 3: Least-Squares Determined Interchain Interaction Constants

| | interaction constants (λ, cm^{-2}/10^3)^a | | |
	a	b	c
orthorhombic *n*-alkanes	0.666 ± 0.02	2.126 ± 0.02	0.206 ± 0.02
monoclinic *n*-alkanes	0.866 ± 0.12	1.916 ± 0.07	0.036 ± 0.09
C-form fatty acids	0.356 ± 0.13	2.066 ± 0.11	0.026 ± 0.07

^{a} Errors estimated in the least-squares determination. The methylene−methylene interaction constants are defined in Figure 3.

monoclinic *n*-alkanes $n = 28$ and 30 at 77 K are from ref 3, and those for $n = 36$ at room temperature are from ref 23. The splittings for the C-form fatty acids $n_{even} = 16-22$ at 10 K listed in Table 2 are our measured values. The fatty acids were also measured at higher temperatures. At 80 K, the splittings are slightly smaller (<0.2 cm^{-1}) than at 10 K. At room temperature, they are about 20% smaller. The reduction in splitting in going to higher temperatures is due to the weaker interchain coupling that accompanies the lateral expansion, which for PM chain layer structures is characteristically large.[21]

Overall, the splitting vs frequency curves in Figure 11 show a sinusoidal-like component that is associated with the *b* term in the equations (19a−c) that relate the splitting to the interaction constants and the phase difference. The effect of this term on the splitting pattern, an effect augmented by the large value of *b* relative to that of *a* and *c*, becomes apparent if written as $8b(\cos \varphi_k \cos \Delta n\varphi_k)$. In this form it is evident that the periodicity is due to the factor $\cos \Delta n\varphi_k$ and that the period is determined by the methylene off-set number Δn.

Figure 12 displays plots of the observed splittings in terms of $\Delta\lambda$ versus $\cos \varphi$, a format that is more relatable to eqs 19a−c, showing more clearly how the splitting is related to the methylene off-set number and the coupling constants. For example, the plot for the orthorhombic *n*-alkanes is nearly linear, with a slope given by the interaction constant *b* and a deviation from linearity determined by *c*. The constant *a* determines where the plot is positioned along the splitting (vertical) axis.

2. Evaluation of the Interchain Coupling Constants. Table 3 lists the values of *a*, *b*, and *c* determined for the orthorhombic and monoclinic *n*-alkanes and C-form fatty acids from a least-squares fitting of the calculated splittings to the measured ones. In Figure 11 to the right, the splittings calculated for each system using eqs 19a−c and the least-squares evaluated interaction constants are plotted against band frequency. Figure 12 shows similar plots, but in terms of $\Delta\lambda_k$ versus $\cos \varphi$. For each system, the shapes of the observed plots are very near those of the calculated.

That the values of the dimensions of the subcells for the orthorhombic and monoclinic *n*-alkanes and the C-form fatty acids are nearly the same would seem to ensure that the interchain interaction constants for these systems would be correspondingly similar. However, Table 3 shows that there are significant differences. Among the factors that may contribute to the differences, we note that the neglect of methylene twisting in our model is probably not one of them, since in that case all three systems would be affected in the same way.

The primary reason for the variation probably lies in our use of observed band frequencies, uncorrected for shifts due to the chain end groups. The calculated values of the interchain interaction force constants for the *n*-alkanes would be most affected because the shifts for the *n*-alkanes are much larger than those for the fatty acids. In discussing the consequences of using uncorrected frequencies, it is useful to express the end group shift in terms of a phase-difference shift rather than a
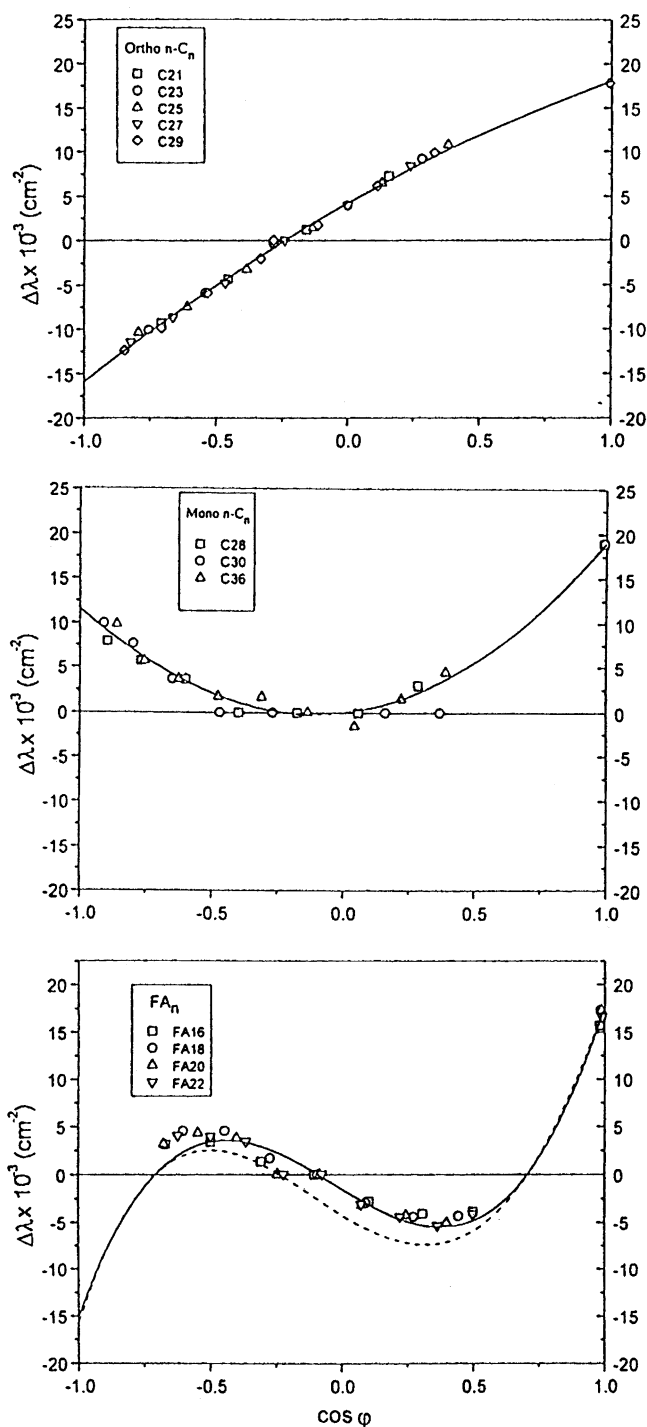

Figure 12. Observed splitting expressed as $\Delta\lambda_k$, plotted against $\cos \varphi$ for the orthorhombic and monoclinic *n*-alkanes and C-form fatty acids. The continuous curves plot the splittings calculated using eqs 19 with interaction constants for each system derived from least-squares fitting (Table 3). The dashed curve for the fatty acids employs splittings based on interaction constants derived for the orthorhombic *n*-alkanes.

frequency shift. The observed frequency/phase-difference plots in Figure 6 indicate the rocking mode phase-difference shift is $5 \pm 1°$ for the *n*-alkanes, but only $1 \pm 1°$ for the fatty acids. The interaction constants evaluated using uncorrected band frequencies will, so to speak, have the phase-difference shift built into them. This is evident in Figure 12 in comparing the two $\Delta\lambda^{calcd}$ vs $\cos \varphi$ plots for the fatty acids. In the solid line plot, the interaction constants used to calculate $\Delta\lambda$ were evaluated using frequencies observed for the C-form fatty acids, which, as noted above, are not much affected by the end groups.
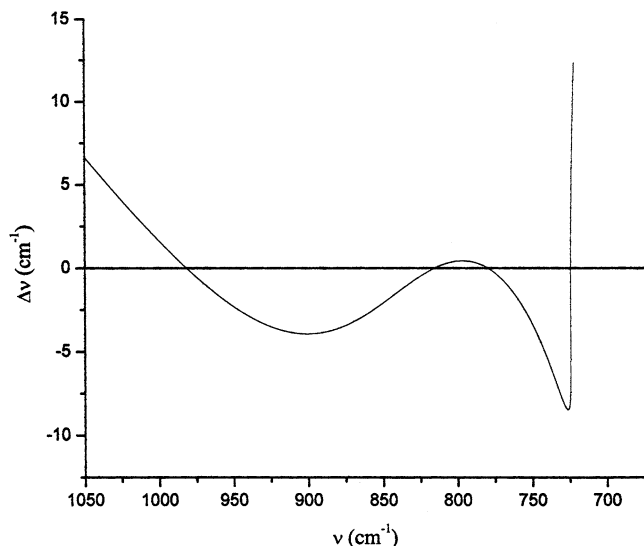
Figure 13. Predicted splitting for $\Delta n = 3$ chain packing, calculated using the coupling constants a, b, and c derived from the orthorhombic n-alkane splitting.

In the dash line plot, the interaction constants used were evaluated using observed frequencies for the n-alkanes, which we know are much more affected by the end groups. The result is a 5° shift between the two curves that matches the 5° shift found in the frequency vs phase-difference plots in Figure 6.

It should be mentioned that the accuracy of the derived values of the interaction constants is reduced by the absence of splitting data in certain frequency regions. The main gap is between 720 and 740 cm^{-1}, where the only splitting that can be measured is that for the intense 720 cm^{-1} band, since all other rocking bands in this region are overlapped by it. The gap is small in terms of frequency, but in terms of the more relevant quantity, the phase difference, it is large, extending from about 10 to 60°. Another gap, also previously mentioned, occurs in the 960−1000 cm^{-1} region of the spectra of the fatty acids, which is overlapped by intense acid group bands.

The best fit between observed and calculated splittings is found for the orthorhombic n-alkanes, because the number of accurately measured splittings is by far the greatest for this system. However, the fitting for the C-form of fatty acids and the monoclinic n-alkanes is nevertheless quite good, good enough to justify displaying in Figure 13 the splitting pattern predicted for chain packing with a methylene off-set number equal to 3. To our knowledge, such a system has thus far not been reported.

Among the interaction constants listed in Table 3, b is largest and the best determined. The value of c is nonzero only for the orthorhombic n-alkanes, in which case it would appear to be well-determined. However, the value of c is suspect because its sign is negative, indicating attraction. In any event, c has by far the smallest value. The value of a is intermediate between b and c.

As discussed in ref 2, the relative values of interaction constants correlate well with the shortest interchain distances between hydrogen pairs associated with the interaction constant. Within the subcell, there are three uniquely short interchain H···H distances. Two of these are associated with b and, together, are responsible for the large value of this constant. The remaining short H···H distance is associated with a. All the H···H distances associated with c are large, which accounts for its small value. As previously noted, the experimentally derived values of the interaction constants for the orthorhombic

n-alkanes are near those calculated using accepted H···H repulsive potentials, confirming that the splitting is due to short-range repulsive interactions mainly between hydrogen atoms.[2,17]

3. Splitting of Near Zone-Center Modes. The splitting observed for the IR active mode at 720 cm^{-1}, whose phase difference is nearest zero, is nearly the same for the orthorhombic and monoclinic n-alkanes phases. For the orthorhombic n-alkanes at 80 K, the measured splitting (averaged over chain lengths $n = 19-25$) is 12.4 ± 0.1 cm^{-1}. The splitting for monoclinic n-alkanes at comparable temperatures and chain lengths is only slightly smaller (<0.2 cm^{-1}) than that for the orthorhombic crystal. The calculated splittings, 12.4 and 12.2 cm^{-1}, for orthorhombic and monoclinic n-C_{20} obtained using eqs 19a and 19b with the interaction constants derived from the orthorhombic n-alkanes are thus in excellent agreement with the observed values. To round out the picture, the calculated splitting for an orthorhombic crystal consisting of infinite PM chains, a structure closely approximated by polyethylene, is 12.5 cm^{-1}. This value is near the 12.4 cm^{-1} calculated for the orthorhombic n-C_{21} and is also near the 12.6 cm^{-1} measured for crystalline polyethylene at 10 K.

Seemingly out of line, the splitting observed for the fatty acids at low temperatures is smaller than that for the orthorhombic n-alkanes by about 1.0 cm^{-1}, a large difference relative to that (<0.2 cm^{-1}) observed in going from the monoclinic to orthorhombic n-alkanes. The possibility that the lower value for the C-form fatty acid crystal results from weaker interchain interactions (a priori unlikely) is in essence ruled out because the decreased splitting can be entirely accounted for as a consequence of the large chain tilt. The observed splitting for the C-form fatty acids at 10 K, averaged over the four homologues, is 11.5 60.2 cm^{-1}. The splitting at 77 K is, within experimental error (±0.2 cm^{-1}), the same as that at 10 K. The calculated splitting for an off-set number of 2 is 11.6 cm^{-1}, in excellent agreement with the observed value.

We have also considered the splitting of the rocking band nearest the 1174 cm^{-1} zone center of the dispersion curve associated with the twisting−rocking band progression that extends from 1380 to 1174 cm^{-1}. The zone center mode at 1174 cm^{-1} represents out-of-phase ($\varphi = \pi$) rocking and is therefore the complement of the zone center in-phase ($\varphi = 0$) mode at 720 cm^{-1} of the rocking−twisting dispersion curve.[4,5]

In applying our model to the twisting−rocking dispersion curve, we have assigned the rocking band nearest the 1174 cm^{-1} zone center as the terminal band in the progression; that is, $k = m$. The relative intensity of this band is very low, and in fact, it is zero for the infinitely long chain, since the zone center mode is IR inactive. We were able to observe it at 1187 cm^{-1} in the spectrum of the shortest of the fatty acids, FA_{16}, because its intensity is enhanced by the acid group. This band is split by ±5.3 cm^{-1} at 10 K. Using in eq 19c the phase difference $\varphi_m = m\pi/(m + 1)$ given by eq 4 and interchain interaction constants derived from the orthorhombic n-alkanes, we calculated a splitting of −5.9 cm^{-1}. Analysis of the other bands in this progression is difficult because of overlapping by a series of more intense bands that belong to the methylene wagging progression. The wagging dispersion curve runs parallel and very near to the twisting−rocking dispersion curve.

4. Chain End Effects on Splitting. Band splitting in the spectra of crystals with tilted chains is subject to chain end perturbations that originate from chain end lateral packing asymmetry. If the chains are tilted, some of the methylenes nearest the chain ends will have as a lateral neighbor a methyl group or a void instead of another methylene. Consequently, a number of interchain
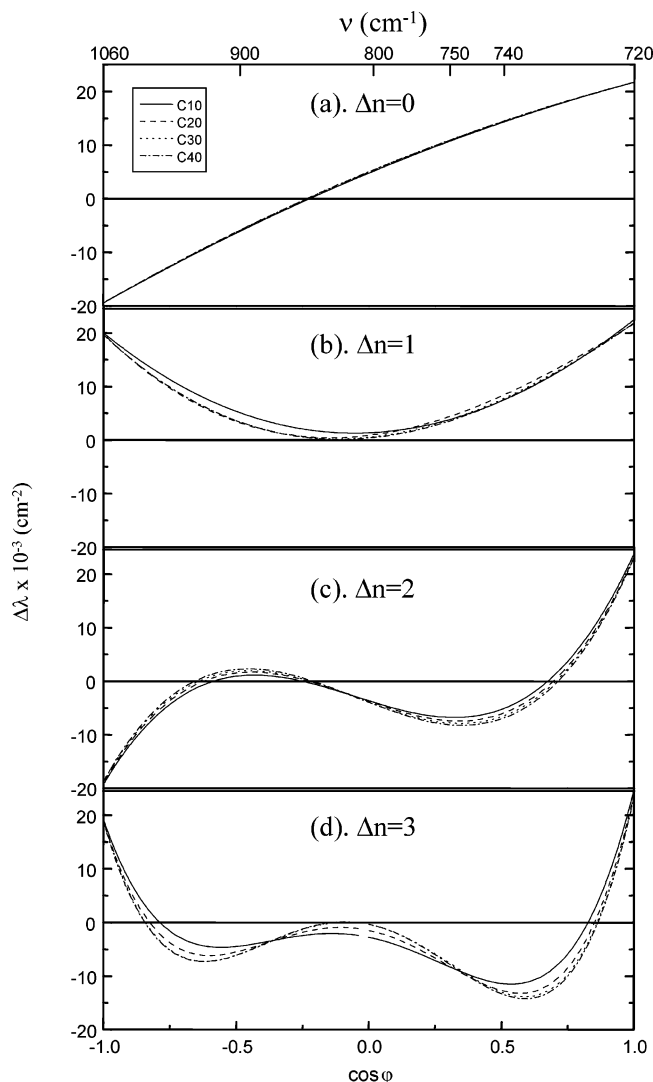
Differences in IR Methylene Rocking Bands

J. Phys. Chem. A, Vol. 108, No. 32, 2004 **6641**

Figure 14. Calculated band splitting $\Delta\lambda$ for the *n*-alkanes and fatty acids, plotted against cos φ for different chain lengths and methylene off-set numbers to illustrate the dependence of interchain end effects on chain tilt and chain length.

methylene−methylene interactions are missing on one side of the chain. The splitting for the C-form fatty acids is most affected because chain tilt is greatest for this system.

To explore the dependence of this effect on chain tilt and chain length, we calculated splittings for chain packing with off-set numbers 0−3, for chains with 40, 30, 20, and 10 methylenes, using the interaction constants evaluated for the orthorhombic *n*-alkanes. The splittings, which were obtained through numerical diagonalization of the h^s matrix defined in eqs 18a−c, are displayed in Figure 14 in $\Delta\lambda$ vs cosφ plots.

Figure 14 shows that, at a fixed tilt, splitting decreases with decreasing chain length. At a length of 40 methylenes, the splitting is only a few tenths of a wavenumber less than that for a chain free of end effects. The effect is quite large for short chains. For example, the calculated splittings for a C-form fatty acid ($\Delta n = 2$) rocking band with a frequency of 740 cm^{-1} ($\varphi = 60°$, cos $\varphi = 0.5$) are −4.8, −4.5, −4.1, and −3.6 cm^{-1} for chain lengths of 40, 30, 20, and 10 methylenes. Thus, the measured splitting for a chain of 10 methylenes is reduced by about 25%. For chains longer than 30 methylenes, the observed splittings are reduced at most by 2%. For our fatty acids, the largest interchain-length effect would then be for FA$_{16}$, whose measured splittings are probably about 20% less than those for

the infinitely long chain. For FA$_{22}$, our longest, the reduction is estimated to be only about 7%. For the monoclinic *n*-alkanes, these effects follow a similar pattern except that their magnitude is about one-half of that for the fatty acids.

Band splitting decreases with increasing tilt, but not linearly. Thus, as may be seen in Figure 14, the overall decrease in the magnitude of the splitting with increasing tilt in going from the monoclinic ($\Delta n = 1$) *n*-alkanes to C-form fatty acids ($\Delta n = 2$) is considerably greater than that estimated in going from orthorhombic ($\Delta n = 0$) to monoclinic *n*-alkanes.

5. Relative Intensities of the Split Band Components. For the fatty acids, the measured values of the ratios of the intensities, A_k^a/A_k^b, of the *a* and *b* components of the split bands vary with *k*. In contrast, for the orthorhombic *n*-alkanes, this ratio is nearly independent of *k* and has a value given by

$$A_k^a/A_k^b = \tan^2 \theta \tag{20}$$

where θ is the setting angle, defined as the angle between the skeletal plane of an *n*-alkane chain and the *a* axis of the subcell as shown in Figure 1. Equation 20 follows from the equality

$$A_k^a/A_k^b = (\partial\mu/\partial Q_k^a)^2/(\partial\mu//\partial Q_k^b)^2 \tag{21}$$

where Q_k^a and Q_k^b are normal coordinates representing the in-phase and out-of-phase combinations of rocking vibration *k* of the two chains in the subcell. The dipole moment derivatives $\partial\mu/\partial Q_k^a$ and $\partial\mu/\partial Q_k^b$ are

$$\partial\mu/\partial Q_k^a = \partial\mu/\partial Q_k^{(1)} + \partial\mu/\partial Q_k^{(2)} \tag{22a}$$

$$\partial\mu/\partial Q_k^b = \partial\mu/\partial Q_k^{(1)} - \partial\mu/\partial Q_k^{(2)} \tag{22b}$$

where $Q_k^{(1)}$ and $Q_k^{(2)}$ are the normal coordinates of rocking mode *k* for molecules 1 and 2. Because the directions of the dipole moment derivatives $\partial\mu/\partial Q_k^{(1)}$ and $\partial\mu/\partial Q_k^{(2)}$ for the all-trans *n*-alkanes are perpendicular to the skeletal plane of the chains, their components along the a_s and b_s axes are proportional to sin θ and cos θ, which leads to eq 20. If we use in eq 20 the value of 42° for the setting angle θ determined for *n*-C$_{23}$ by X-ray diffraction,[14] we find $A_k^a/A_k^b = 0.9$ for the orthorhombic *n*-alkanes. This value is in accord with the measured intensity ratios[2].

Of the approximately 25 rocking bands that appear in the four spectra of the C-form fatty acids for which it is possible to estimate A_k^a/A_k^b, about two-thirds are within 20% of the observed average for the orthorhombic *n*-alkanes. It can be assumed that the modes associated with this two-thirds have normal coordinates similar to those of the *n*-alkanes. That is, the motion involved is primarily methylene rocking. The deviant values can be assumed to involve modes with a significant contribution from the acid group. Because of interchain hydrogen bonding, the plane of the acid group is unlikely to be parallel to the plane of the PM chain, so that eq 20 is not applicable to the fatty acids.

Supporting Information Available: Figures 1S, 2S, and 3S. Figure 1S shows observed IR intensities of the rocking mode bands for the C-form fatty acids and the orthorhombic *n*-alkane *n*-C$_{21}$ at 10 K plotted against the phase difference. Figure 2S shows the rocking fraction of the vibrational eigenfunction based

on the fraction of potential energy from methylene rocking plotted against phase difference. Figure 3S shows observed and calculated dipole moment derivatives for the rocking bands of n-C_{21} at 10 K, plotted against phase difference. This material is available free of charge via the Internet at http://pubs.acs.org.

References and Notes

(1) Snyder, R. G. *J. Phys. Chem.* **1957**, *27*, 969.

(2) Snyder, R. G. *J. Mol. Struct.* **1961**, *7*, 116.

(3) Snyder, R. G. *J. Chem. Phys.* **1979**, *71*, 3229.

(4) Snyder, R. G.; Schachtschneider, J. H. *Spectrochim. Acta* **1963**, *19*, 85.

(5) Schachtschneider, J. H.; Snyder, R. G. *Spectrochim. Acta* **1963**, *19*, 117.

(6) Hadzi, D.; Sheppard, N. *Proc. R. Soc. London, Ser A* **1953**, *216*, 247.

(7) Matsuda, H.; Okada, K.; Takase, T.; Yamamoto, T. *J. Chem. Phys.* **1964**, *41*, 1527.

(8) Uno, T.; Machida, K. *Spectrochim. Acta* **1968**, *24*, 1741.

(9) Snyder, R. G. *J. Mol. Spectrosc.* **1967**, *23*, 224.

(10) Yan, W. H.; Strauss, H. L.; Snyder, R. G. *J. Phys. Chem.* **2000**, *B104*, 4229.

(11) Snyder, R. G. *J. Chem. Phys.* **1965**, *42*, 1744.

(12) Wilson, E. B.; Decius, J. C.; Cross; P. C. *Molecular Vibrations*; McGraw-Hill: New York, 1955; Chapter 7.

(13) Abrahamsson, S.; Dahlen, B.; Lofgren, H.; Pascher, I. *Prog. Chem. Fats Other Lipids* **1978**, *16*, 125.

(14) Smith, A. E. *J. Chem. Phys.* **1953**, *21*, 2229.

(15) Thompson, H. W.; Torkington, P. *Proc. R. Soc. London, Ser. A.* **1945**, *184*, 3.

(16) Stein, R. S. *J. Chem. Phys.* **1955**, *23*, 743.

(17) Tasumi, M.; Shimanouchi, T. *J. Chem Phys.* **1965**, *43*, 1245.

(18) Snyder, R. G.; Goh, M. C.; Srivatsavoy, V. J. P.; Strauss, H. L.; Dorset D. L. *J. Phys. Chem.* **1992**, *96*, 10008.

(19) Snyder, R. G.; Strauss, H. L.; Cates, D. A. *J. Phys. Chem.* **1995**, *99*, 8432.

(20) Mendelsohn, R.; Liang, G. L.; Strauss, H. L.; Snyder, R. G. *Biophys. J.* **1995**, *69*, 987.

(21) Small, D. M. *The Physical Chemistry of Lipids*; Plenum Press: New York, 1986.

(22) Vand, V.; Morely, W. M.; Lomer, T. R. *Acta Crystallogr.* **1951**, *4*, 324.

(23) Holland, R. F.; Nielsen, J. R. *J. Mol. Struct.* **1962**, *8*, 383.